

## BiCu<sub>2</sub>VO<sub>6</sub>: a new narrow-band spin-gap material

T. MASUDA<sup>1</sup>, A. ZHELUDEV<sup>1</sup>, H. KAGEYAMA<sup>2</sup> and A. N. VASILIEV<sup>2,3(\*)</sup>

<sup>1</sup> *Condensed Matter Science Division, Oak Ridge National Laboratory, Oak Ridge, TN 37831-6393, USA*

<sup>2</sup> *Institute for Solid State Physics, University of Tokyo, 5-1-5 Kashiwanoha, Kashiwa, Chiba 277-8581, Japan*

<sup>3</sup> *Department of Low Temperature Physics M.V. Lomonosov Moscow State University Moscow 119899 Russia*

PACS. 75.10.Pq – Spin chain models .

PACS. 75.30.Ds – Spin waves .

PACS. 75.30.Et – Exchange and superexchange interactions .

**Abstract.** – A new spin-ladder family material BiCu<sub>2</sub>VO<sub>6</sub> is studied by means of the magnetic susceptibility, heat capacity and neutron inelastic scattering measurements on powder sample. Singlet ground state and a finite spin gap are confirmed by thermal-activated type susceptibility and by distinct peak at 16 meV in spin excitation. Triple narrow band structure in spin excitation spectrum, probably due to complex crystal structure, is observed and the possibility of weakly-interacting spin-cluster system is discussed.

*Introduction.* – In recent years quantum antiferromagnets with an intrinsically disordered (“spin liquid”) ground state and energy gap in the spin excitation spectrum have received a great deal of attention [1, 2, 3, 4]. Among the simplest materials of this type are weakly interacting singlet spin clusters, such as dimers, spin-rings or plaquettes. The bandwidth of spin excitations from disordered ground state, what we will call “magnons” hereafter, in such materials are typically smaller or comparable to the gap energy. This feature make them attractive to both theorists and experimentalists. In many cases, inter-cluster interactions are sufficiently weak to be studied perturbatively, yet strong enough to give rise to complex cooperative phenomena are found in wide-band systems, such as spin chains and spin ladders. Many prototypical coupled-dimer materials turned out to be particularly interesting from this point of view. Among the more extensively studied systems are the alternating chain compound VODPO [5], the spin-bilayer material BaCuSi<sub>2</sub>O<sub>6</sub> [6], and the Shastry-Sutherland [7] material SrCu<sub>2</sub>(BO<sub>3</sub>)<sub>2</sub> [8]. Neutron scattering experiments on Cu(NO<sub>3</sub>)<sub>2</sub>·2.5D<sub>2</sub>O [9] revealed not only dispersive single-dimer modes, but also a highly structured continuum of multi-dimer excitations. Another interesting case is that of (Tl,K)CuCl<sub>3</sub> [10, 11, 12, 13, 14], where antiferromagnetic long-range order has been induced by a strong external magnetic field, pressure, or impurity doping.

---

(\*) Permanent address is Low Temperature Physics Department, Moscow State University, Moscow 119992, Russia

In our search for new experimental realizations of spin-ladder and related models, we came across a new interesting family of low-dimensional materials with the general formula  $\text{BiCu}_2\text{AO}_6$  ( $A = \text{V}$  [15],  $\text{P}$  [16], and  $\text{As}$  [17]). As will be shown in the present paper, at least one of these compounds, namely  $\text{BiCu}_2\text{VO}_6$ , indeed has a non-magnetic singlet ground state and a gap in the spin excitation spectrum.

The crystal structure of  $\text{BiCu}_2\text{VO}_6$  is of relatively low symmetry, monoclinic, space group  $P2_1/n$  [15], and is schematically visualized in Fig. 1 (a). Lattice parameters are  $a = 13.49 \text{ \AA}$ ,  $b = 7.822 \text{ \AA}$ ,  $c = 15.79 \text{ \AA}$ , and  $\beta = 113.113^\circ$ . The most prominent feature are zig-zag ladder structures formed by the  $S = 1/2$ -carrying  $\text{Cu}^{2+}$ , assumed to be responsible for the magnetic properties. The ladders run along the crystallographic  $c$ -axis and are separated by non-magnetic  $\text{V}^{5+}$  and  $\text{Bi}^{3+}$  ions. The rung of the ladders are roughly parallel to the crystallographic  $b$ -direction. As shown in Fig. 1 (b), the ladders actually incorporate six *inequivalent* Cu-sites, which results in eight *inequivalent* Cu-O-Cu bond. Given the location of  $\text{O}^{2-}$  ions that are likely to play a key role in superexchange interactions in this material, one can hypothesize a spin Hamiltonian with up to eight unequal exchange parameters (Fig. 1 (b)). Even though crystallographic considerations point towards a quasi-one-dimensional distorted ladder-type system, we find that  $\text{BiCu}_2\text{VO}_6$  possesses all the features of a narrow-band “cluster” model, possibly composed of weakly interacting dimers.

*Experimental Procedure and Results.* – The non-magnetic nature of the ground state and the energy gap in  $\text{BiCu}_2\text{VO}_6$  were detected in bulk susceptibility measurements. These data were collected using a Quantum Design SQUID magnetometer on a powder sample in a 1000 Oe field, and are shown in Fig. 2 (a). Apart from the low-temperature upturn that is most likely due to impurities, the susceptibility curve has a pronounced thermal-activated character. As a point of reference, it can be approximated by a  $S = 1/2$  dimer susceptibility curve, with an additional Curie contribution at low temperatures due to impurities. The result of such fit shown in a solid line in 2 (a). In plotting this curve we used the value  $g = 2.03$  for the gyromagnetic ratio of  $\text{Cu}^{2+}$ , as determined by room-temperature ESR measurements. The fitted a singlet-triplet dimer splitting is  $\Delta 16 \text{ meV}$ . The amount of impurity was estimated to be only 0.8% of  $\text{Cu}^{2+}$  ions. While this simplest local-singlet models is probably an inappropriate description of  $\text{BiCu}_2\text{VO}_6$ , the extracted gap energy sets the characteristic magnitude of spin interactions.

Due to the large magnetic energy scales involved, the magnetic contribution to heat capacity is too weak to be isolated from the phonon part. This fact is borne out in Figure 2 (b) that shows the  $C(T)$  curve measured in a “Termis” calorimeter using the quasiadiabatic method on a polycrystalline sample a polycrystal sample (circles), in comparison with that calculated for the dimer model described above (solid line). One useful piece of information that is contained in the specific heat data, is the absence of any signatures of phase transitions over a temperature range 6.4 - 260 K. This supports the notion that the non-magnetic ground state is an intrinsic property of the spin network as it is at room temperature, and not a result of some structural transition.

More insight into the nature of the ground state and magnetic gap excitations was obtained in inelastic neutron scattering experiments on  $\text{BiCu}_2\text{VO}_6$ . The data were collected on a 14.5g powder sample using the HB-1 3-axis spectrometer installed at the High Flux Isotope Reactor at Oak Ridge national Laboratory. Neutrons of a fixed final energy  $E_f = 13.5 \text{ meV}$  were used in combination with a graphite filter positioned after the sample. Soller collimators defined the neutron beam divergencies as  $48' - 60' - 60' - 120'$ . Sample environment was a standard closed-cycle refrigerator.

Typical constant- $Q$  scans collected at  $T = 10 \text{ K}$  are shown in Fig. 3. A number of such

scans were combined to produce the false-color plot shown in Fig. 4. Inelastic powder data are notoriously difficult to interpret due to the spherical averaging that is an intrinsic feature of powder scattering. In our case of BiCu<sub>2</sub>VO<sub>6</sub> the situation is even more complicated than usual, largely due to the energy scales involved. The powder-averaged dynamic structure factor is most informative at small momentum transfers, where the averaging occurs across only a few Brillouin zones, and where the signal often has a lot of “structure”. A good example of such behavior was witnessed in recent powder experiments on the Haldane-gap antiferromagnet PbNi<sub>2</sub>V<sub>2</sub>O<sub>8</sub> [18, 19, 20]. In the present study however, momentum transfers below 1 Å<sup>-1</sup> are unreachable in the interesting energy transfer range (15 to 40 meV) due to kinematic constraints [21]. At higher wave vectors, any characteristic features of the cross section are progressively “smeared” by spherical averaging over several Brillouin zones. Magnetic scattering then becomes similar to the magnon density of states function. Moreover, the background, largely due to inelastic incoherent scattering by phonons that involve the V-nuclei, becomes progressively stronger at higher momentum transfers, while magnetic scattering is suppressed due to the magnetic form factor.

Given these intrinsic limitations of the present powder experiment and the complexity of the crystal structure and geometry of magnetic interactions, a quantitative analysis of the data, similar to the one described in Refs. [18, 19, 20] does not appear feasible. The data obtained in our neutron experiments can nevertheless provide some qualitative clues to the nature of the singlet ground state and energy gap in BiCu<sub>2</sub>VO<sub>6</sub>. The most prominent feature of the inelastic scattering, clearly visible in Fig. 4, are three bands of intensity at energy transfers 16 meV, 25 meV, and 39 meV, respectively. The central energies were determined in Gaussian fits as those shown in solid lines in Fig. 3. Overall, in the admittedly narrow  $q$ -range sampled, there is very little wave vector dependence to scattering. As shown in Fig. 3, only the lower peak is somewhat broader than the experimental energy resolution (intrinsic width 3.2 meV FWHM), and the two higher-energy features are resolution-limited. The 16 meV peak is clearly to be associated with the energy gap in the system.

*Discussion.* – There are at least two alternative explanations for the observed intensity bands. One possibility is that the scattering is due to a single dominant magnon branch with a rather wide dispersion bandwidth between the gap energy of  $\Delta \approx 16$  meV and a zone-boundary energy of 39 meV. The three peaks are then associated with Van Hove singularities in the magnon density of states. The location and intensity of the peaks primarily depends on the details of the magnon dispersion relation. Such is the case for powder experiments on several materials including PbNi<sub>2</sub>V<sub>2</sub>O<sub>8</sub>. [18, 19, 20, 22, 23] A different explanation attributes the three observed peaks to three distinct branches of narrow-band singlet-triplet excitations in one or more local spin clusters, such as dimers. For BiCu<sub>2</sub>VO<sub>6</sub> this explanation seems to be the more likely one. Indeed the measured powder spectrum (Fig. 3) has many similarities with that seen in the well-characterized isolated-dimer material [24] (See Fig. 4 in Ref. [24]). The observed  $q$ -dependence is a slowly varying function that may represent smooth oscillations of the single-cluster structure factor, rather than sharp features expected from powder-averaging of magnon cross sections with a steep dispersion [18, 19, 20, 22, 23]. In the local-cluster interpretation the intrinsic width of the 16 meV peak in BiCu<sub>2</sub>VO<sub>6</sub> is attributed to weak interactions between the clusters, the magnon bandwidth being directly related to the apparent energy width of the intensity band in the powder data. The symmetry of BiCu<sub>2</sub>VO<sub>6</sub> is low enough to allow up to three different dimer types, based on the 6 inequivalent Cu<sup>2+</sup> positions. Other possibilities may include 4- and even 6-spin clusters. Lacking a reliable model of magnetic interactions in BiCu<sub>2</sub>VO<sub>6</sub>, a further exploration of this avenue will have to be postponed until single crystal samples become available.

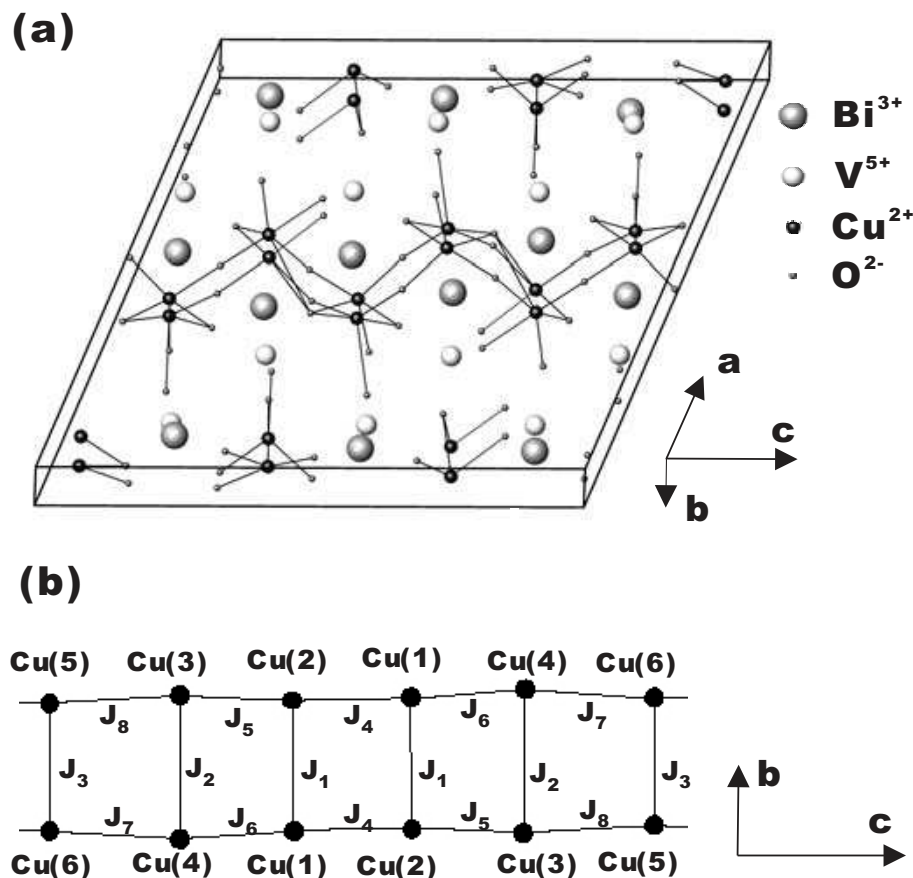


Fig. 1 – (a) Crystal structure of  $\text{BiCu}_2\text{VO}_6$ .  $S = 1/2$  carrying  $\text{Cu}^{2+}$  ions form zig-zag ladder along the crystallographic  $c$  axis, which is separated by non-magnetic  $\text{Bi}^{3+}$  and  $\text{V}^{5+}$  ions. (b) Framework of  $\text{Cu}^{2+}$  ions projected onto  $b - c$  plane. Six inequivalent  $\text{Cu}^{2+}$  ions suggests eight different exchange interaction in distorted ladder structure.

*Conclusion.* – There are two lessons to be learned from our experiments on  $\text{BiCu}_2\text{VO}_6$  powder samples. First, we have shown that at least one member of the  $\text{BiCu}_2\text{AO}_6$  family is a singlet ground state material, and identified the underlying ladder-type spin arrangement. Second, it became obvious that the main obstacle to fully understanding the physics of  $\text{BiCu}_2\text{VO}_6$  is in its distorted and complicated crystal structure. Other members of the family, for example  $\text{BiCu}_2\text{PO}_6$  may be more valuable as model quantum magnets, since their structure features undistorted spin ladders.

*Acknowledgements.* – We thank Dr. E. Popova for assistance in specific heat measurements and Dr. Y. Petrusevich and Dr. Y. Koksharov for taking ESR spectra at room temperature. Work at ORNL was carried out under Contracts No. DE-AC05-00OR22725, US Department of Energy. Work at ISSP was supported by the MECSST (Japan) through Grant-in-Aid for Scientific Reserach No. 40302640. A.N.V. acknowledge support through RFBR Grant 03-02-16108 and NWO Grant 008-012-047.

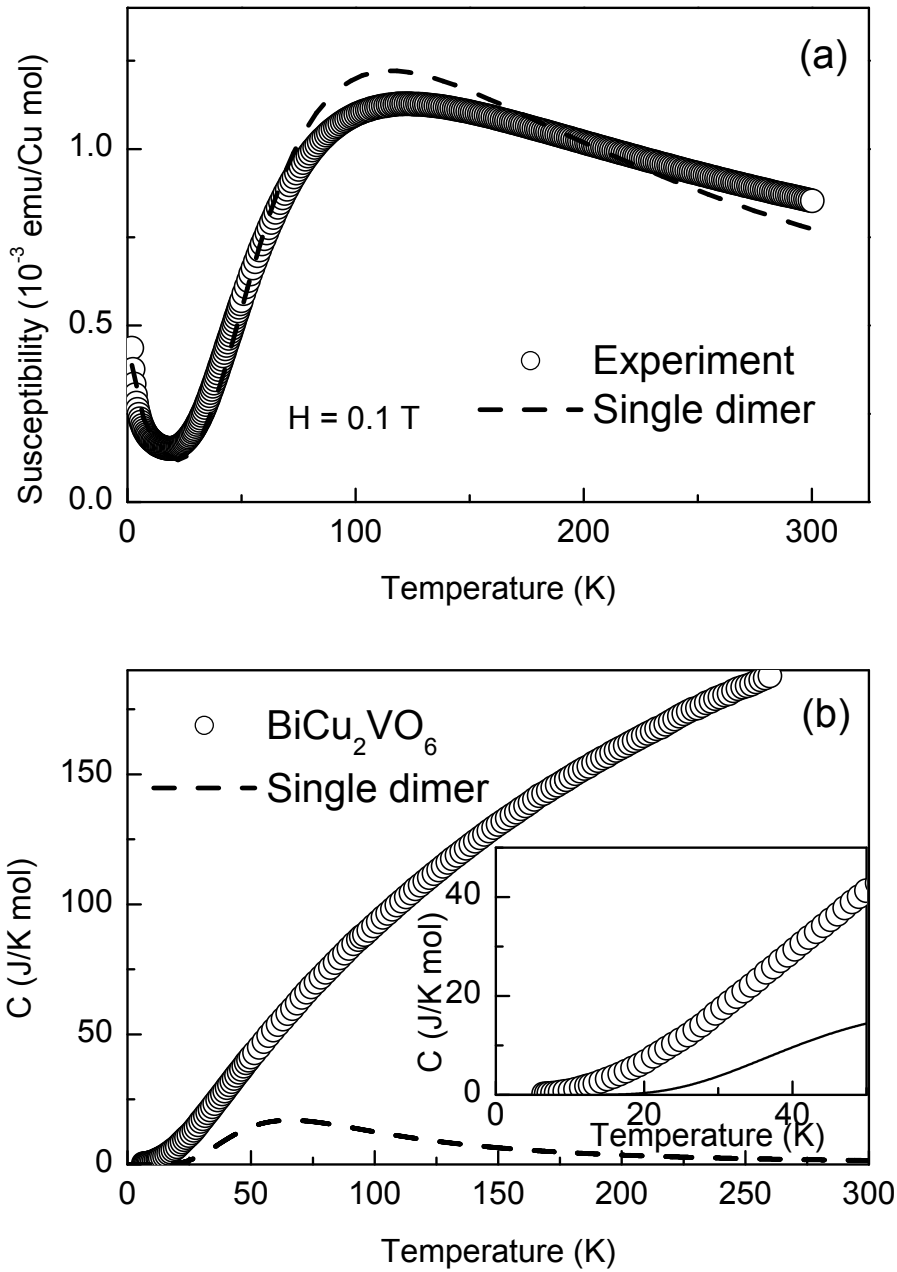


Fig. 2 – (a) Magnetic susceptibility (open circle) and fit by spin-dimer model (dashed line). The thermal-activated feature suggests the singlet ground state and a finite spin gap. Applied field is 0.1 T and a temperature range is 2 - 300 K. (b) Heat capacity (open circle) and spin-heat capacity predicted by spin-dimer model (dashed line). No signature of phase transition is observed. Applied field is 0 T and a temperature range is 6.4 - 260 K

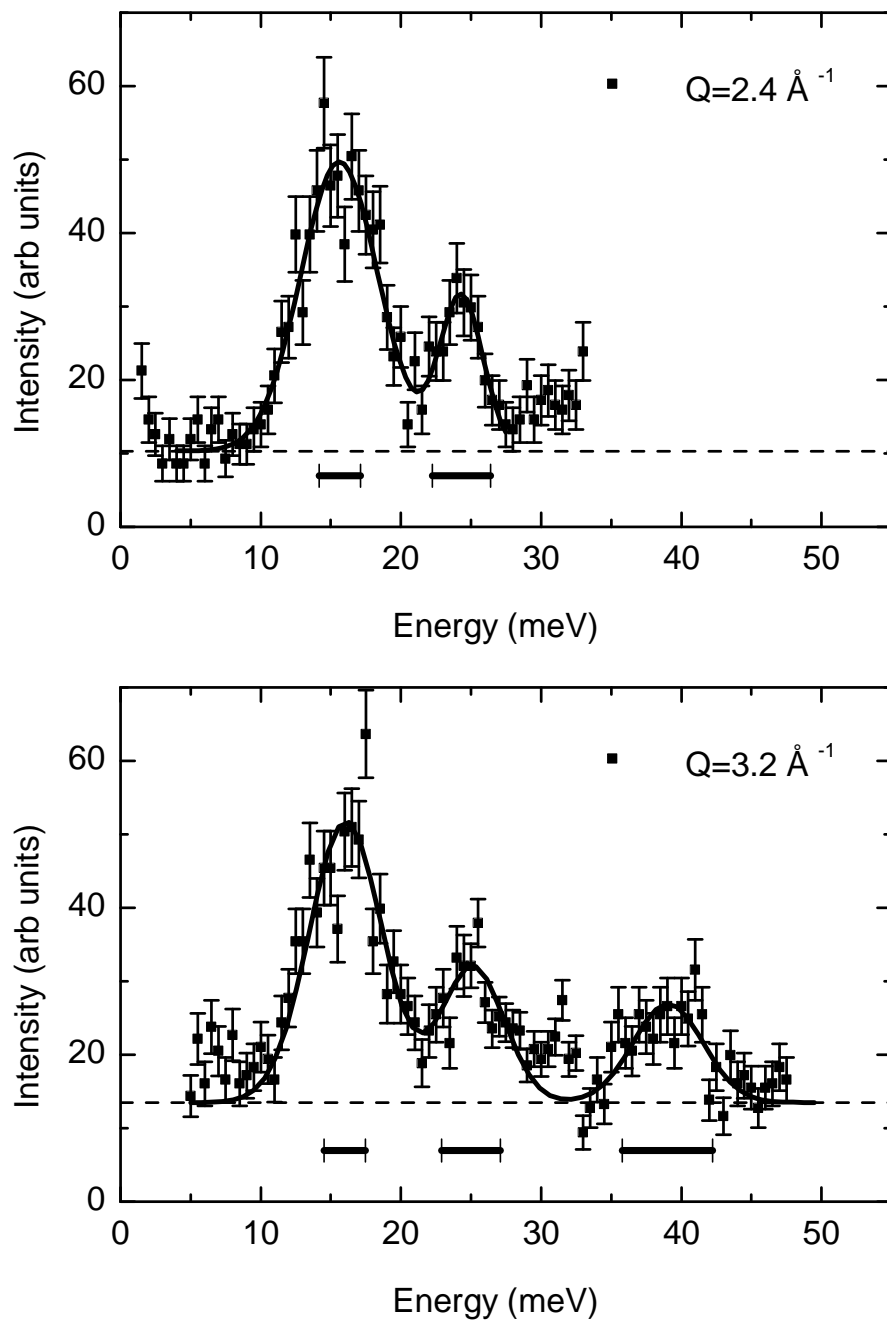


Fig. 3 – Constant  $Q$  scan at  $2.4 \text{ \AA}^{-1}$  and  $3.2 \text{ \AA}^{-1}$ . Solid line is fit by multi Gaussian, dotted line is background from the fit, bars are resolution in energy. Distinct peaks are observed at 16, 25, and 39 meV. The peak at 16 meV has intrinsic finite width while those at 25 and 39 meV are in resolution limit.

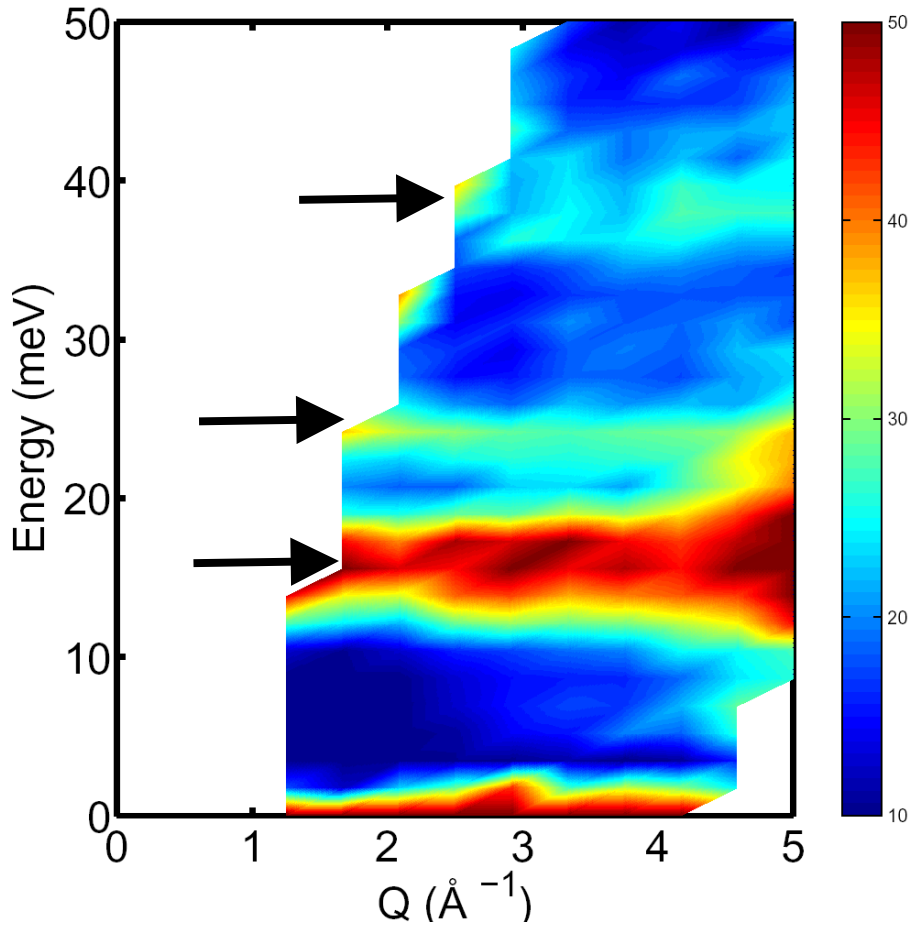


Fig. 4 – Energy vs  $Q$  false color map. Triple narrow bands are indicated by arrows. The absence of intensity below lowest energy band at 16 meV means the existence of bound state there and intrinsic spin gap in this material. Triple band structure is discussed in the text.

#### REFERENCES

- [1] HALDANE F. D. M., *Phys. Rev. Lett.*, **50** (1983) 1153.
- [2] DAGOTTO E., RIERA J. and SCALAPINO D., *Phys. Rev. B*, **45** (1992) 5744.
- [3] RICE T. M., GOPALAN S. and SIGRIST M., *Europhys. Lett.*, **23** (1993) 445.
- [4] HASE M., TERASAKI I. and UCHINOKURA K., *Phys. Rev. Lett.*, **70** (1993) 3651.
- [5] GARRETT A. W., NAGLER S. E., TENNANT D. A., SALES B. C. and BARNES T., REVIEW-*Phys. Rev. Lett.* 791997745
- [6] SASAGO Y., UCHINOKURA K., ZHELUDEV A. and SHIRANE G., *Phys. Rev. B*, **55** (1997) 8357.
- [7] SHASTRY B. S. and SUTHERLAND B., *Physica*, **108B** (1981) 1069.
- [8] KAGEYAMA H., YOSHIMURA K., STERN R., MUSHNIKOV N. V., ONIZUKA K., KATO M., KOSUGI K., SLICHTER C. P., GOTO T. and UEDA Y., *Phys. Rev. Lett.*, **82** (1999) 3168.
- [9] XU G., BROHOLM C., REICH D. H. and ADAMS M. A., *Phys. Rev. Lett.*, **84** (2000) 4465.

- [10] OOSAWA A., ISHII M. and TANAKA H., *J. Phys.: Condens. Matter*, **11** (1999) 265.
- [11] CAVADINI N., RÜEGG CH., FURRER A., GÜDEL H. -U., KRÄMER K. MUTKA H. and VORDERWISCH P., *Phys. Rev. B*, **65** (2002) 132415
- [12] OOSAWA A., ONO T. and H. TANAKA, *Phys. Rev. B*, **66** (2002) 020405.
- [13] OOSAWA A., TAKAMATSU T., TATANI K., ABE H., TSUJII N., SUZUKI O., TANAKA H., KIDO G., and KINDO K., *Phys. Rev. B*, **66** (2002) 104405
- [14] OOSAWA A., FUJISAWA M., OSAKABE T., KAKURAI K., and TANAKA H., cond-mat/0301577
- [15] RADOSAVLJEVIC I., EVANS J. S. O. and SLEIGHT A. W., *J. Solid State Chem.*, **141** (1998) 149.
- [16] ABRAHAM F., KETATNI M., MAIRESSE G. and MERNARI B., *Eur. J. Solid State Inorg. Chem. t.*, **31** (1994) 313.
- [17] RADOSAVLJEVIC I., EVANS J. S. O. and SLEIGHT A. W., *J. Alloys and Compounds*, **284** (1999) 99.
- [18] UCHIYAMA Y., SASAGO Y., TSUKADA I., UCHINOKURA K., ZHELUEV A., HAYASHI T., MIURA N. and BÖNI P., *Phys. Rev. Lett.*, **83** (1999) 632
- [19] ZHELUEV A., MASUDA T., TSUKADA I., UCHINOKURA K., BÖNI P., LEE S.-H.,, *Phys. Rev. B*, **62** (2000) 8921
- [20] ZHELUEV A., MASUDA T., UCHINOKURA K. and NAGLER S. E., *Phys. Rev. B*, **64** (2001) 134415
- [21] Kinematics constraints,  $\delta E = \frac{\hbar}{2m}(2\mathbf{k}_i \cdot \mathbf{q} + q^2)$ , restricts the maximum energy transfer small at small  $q$ . Here  $\delta E$  is energy transfer,  $\mathbf{k}_i$  is wave vector of incident neutron,  $\mathbf{q}$  is scattering vector, and  $m$  is the mass of neutron.
- [22] DITUSA J. F., CHEONG S. -W., PARK J. -H., AEPPLI G., BROHOLM C. and CHEN C. T., *Phys. Rev. Lett*, **73** (1994) 1857
- [23] DITUSA J. F., CHEONG S. -W., BROHOLM C., AEPPLI G., RUPP JR. L. W. and BATLOGG B. , *Physica B*, **194-196** (1994) 181
- [24] TENNANT D. A., NAGLER S. E., GARRETT A. W., BARNES T. and TORARDI C. C., *Phys. Rev. Lett.*, **78** (1997) 4998